Sintering of Ultrathin Gold Nanowires for Transparent Electronics

Johannes H. M. Maurer, Lola González-García, Beate Reiser, Ioannis Kanelidis, and Tobias Kraus

ACS Applied Materials & Interfaces 7 (15)

It has been published in final form at http://dx.doi.org/10.1021/acsami.5b02088.

Sintering of Ultrathin Gold Nanowires for Transparent Electronics

Johannes H.M. Maurer, Lola González-García,* Beate Reiser, Ioannis Kanelidis, and Tobias Kraus*

INM - Leibniz Institute for New Materials, Campus D2 2, 66123 Saarbrücken, Germany

E-mail: lola.gonzalez-garcia@inm-gmbh.de; tobias.kraus@inm-gmbh.de

Abstract

Ultrathin gold nanowires (AuNWs) with diameters below 2 nm and high aspect ratios are considered a promising base material for transparent electrodes. To achieve the conductivity expected for this system, oleylamine must be removed. Herein we present the first study on conductivity, optical transmission, stability, and structure of AuNW networks before and after sintering with different techniques. Freshly prepared layers consisting of densely packed AuNW bundles were insulating and unstable, decomposing into gold spheres after few days. Plasma treatments increased conductivity and stability, coarsened the structure, and left optical transmission virtually unchanged. Optimal conditions reduced sheet resistances to 50 Ω/sq.

Keywords: metal nanostructures, capping ligands, ultrathin gold nanowires, AuNW layers, transparent electronics, soft-sintering, GISAXS

Transparent conductive materials (TCMs) are indispensable components of modern electronic devices such as thin-film displays, transparent solar cells, and touch screens. Most

*To whom correspondence should be addressed

commonly encountered today is indium tin oxide (ITO), which combines large optical transmittances of $T \approx 90\%$ with low sheet resistances in the range of $R_{sheet} \approx 10\ \Omega/\mathrm{sq}$.[1] Indium tin oxide and other transparent oxides have limitations when it comes to flexible and organic electronics, mainly due to their ceramic brittleness and high-temperature vacuum deposition. New classes of TCMs that could replace oxides in such applications include carbon nanotube (CNTs) networks,[2] graphene,[3] metal grids[4] and metallic nanowire networks.[5] Metallic nanowires networks combine high conductivity with mechanical flexibility and can be deposited from liquid dispersions.[6] Silver nanowires (AgNWs)[7] and copper nanowires (CuNWs)[8] networks have been extensively studied and are now commercially competing with ITO.[9]

Since their first synthesis in 2007, ultrathin gold nanowires (AuNWs) with diameters below 2 nm[10–13] and high aspect ratios (>1000) have attracted great interest due to their mechanical flexibility[14,15] and high optical transparency.[16] Gold is more stable towards chemical degradation than silver and copper while its conductivity achieves comparable values.[17] Sanchez-Iglesias et al.[16] and Chen et al.[15] prepared very thin conductive layers from AuNWs with high optical transparency (T>95%), proving the suitability of AuNWs as transparent conductive materials.

The conductivity of nanoparticle-based TCMs is often dominated by contact resistances between individual particles.[18,19] Large resistances are caused by common capping ligands that surround the particles during synthesis and lend them colloidal stability. Isolating ligands act as tunnel barriers and hinder electron transport from particle to particle. For example, AuNWs are capped with oleylamine during synthesis, a molecule that is known to cause high junction resistances.[19] They are the main reason for AuNW films not to reach theoretically predicted conductivities.[15] Although the amount of oleylamine can be lowered by repeated washing of the AuNWs suspension after synthesis, a certain amount of residual oleylamine is necessary to stabilize the thin structures in solution.[20]

Annealing is widely employed to lower the junction resistance in metal particle networks

and to decrease the sheet resistance after layer formation. Thermal annealing,[21] plasma treatment[22,23] and ligand exchange[19,24] have been reported to be effective treatments. However, not all of them are suitable for ultrathin gold wires. Thermal annealing, which has successfully been applied to AgNWs,[21] would require temperatures far beyond the stability limit of AuNWs to remove the high-boiling oleylamine (bp=350°C). Due to their small diameters, AuNWs are extremely vulnerable to fragmentation by Rayleigh instability, which accelerates with increasing temperature.[25–28] Reducing or oxidizing plasmas have been successfully used to remove organic compounds in nanoparticle systems.[22,23] A chemical alternative are ligand exchange reactions in the dry film after deposition. Recently, Fafarman and coworkers[19,24] reported the exchange of the oleylamine on spherical gold nanocrystals by ammoniumthiocyanate (NH_4SCN). They observed a clear dielectric-to-metal transition after oleylamine was replaced by the short, inorganic NH_4SCN. These methods have not been applied to ultrathin gold nanowires so far.

In the following, we present a systematic study on the influence of reducing (5% H_2 in Ar, further referred as hydrogen plasma) and oxidizing (pure O_2) plasma treatment and ligand exchange on structure, conductivity and stability of ultrathin AuNW layers. We discuss the stability of the layers over time as a function of annealing parameters.

A Transmission Electron Microscopy (TEM) image of the as-synthesized ultrathin AuNWs is shown in Figure 1a. The wires had diameters of 1.6 nm, lengths of several micrometers, and a surface-to-surface spacing of around 3 nm. A homogeneous monolayer on the metal core should lead to a surface-to-surface spacing of 2-4 nm due to the interdigitation of the oleylamine molecules as reported in literature.[29] We deposited AuNW layers with a thickness of approximately 10 nm on glass by dip coating (see Methods in the Supporting Information). A representative Scanning Electron Microscopy (SEM) image of an as-deposited layer is shown in Figure 1b. Dense layers composed of AuNW "bundles" that were visible in SEM formed.[15] The photograph in Figure 1b shows the characteristic color of fresh layers that is due to the surface plasmon resonance of the gold nanowires. Corresponding transmittance

spectra can be found in the Supporting Information (Figure S1).

Individual AuNWs are hardly visible in scanning electron micrographs. To investigate the wire arrangement in the layer, Grazing Incidence Small-Angle X-ray Scattering (GISAXS) measurements were performed. The pattern shown in Figure 1c indicates the presence of single wires. The peaks at $q_y = \pm 1.5$ nm^{-1} (see horizontal intensity profile in Figure 1d) correspond to the average center-to-center distance of 4.2 nm.

Freshly deposited AuNW layers exhibited sheet resistances >40 MΩ, a value that is probably dominated by oleylamine tunnelling barriers between the metal nanostructures.

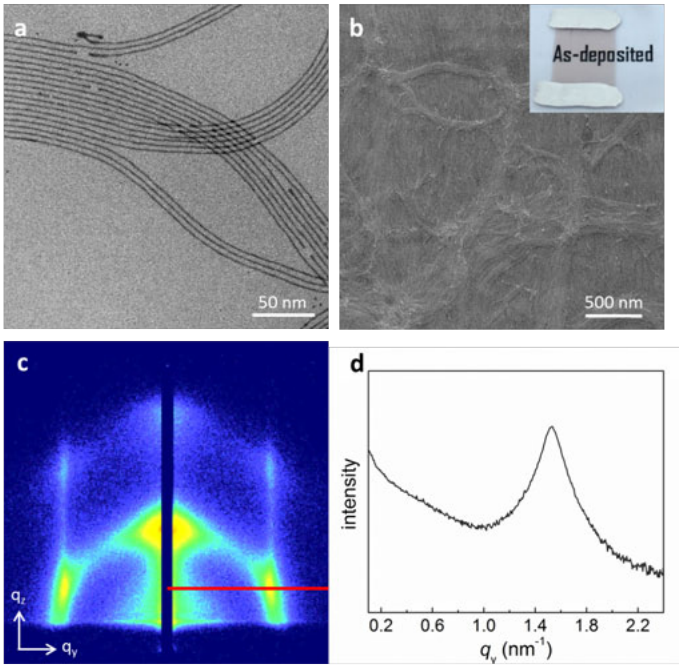

Figure 1: (a) Transmission electron micrograph of single gold nanowires and (b) scanning electron micrograph of a dense AuNW layer on glass as used in this work. The inset shows a photograph of the layer. (c) Grazing incidence small-angle X-ray scattering pattern of an as-deposited AuNW layer. (d) Intensity distribution along the red bar in panel (c).

Figure 2 shows SEM images and sheet resistances after exposure to hydrogen plasma, oxygen plasma and ammoniumthiocyanate solution. Plasma treatments readily decreased sheet resistances down to the ohm range, while immersion in ammoniumthiocyanate solution only decreased them to tens of megaohms, even after prolonged immersion.

Hydrogen plasma exposure for 1 minute did not significantly change the appearance of

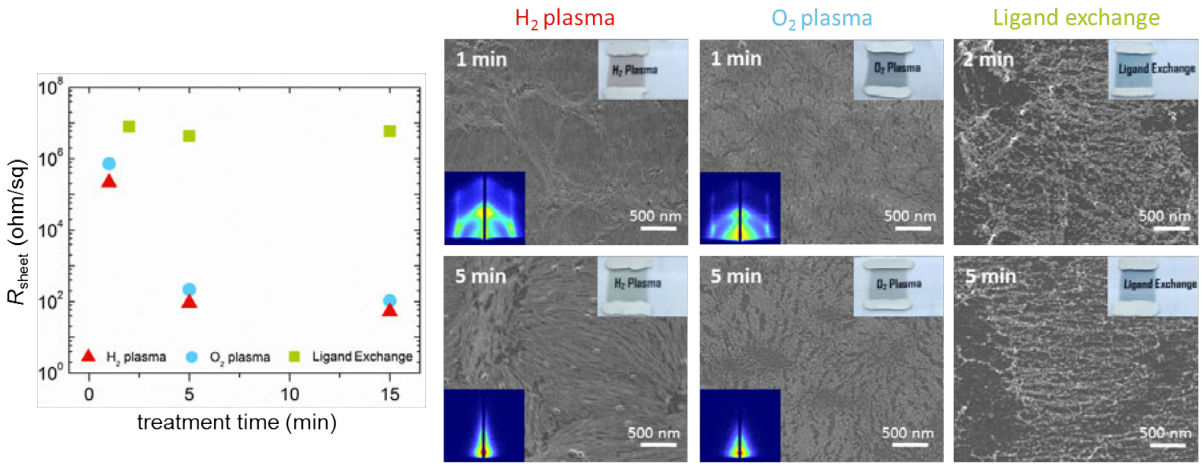

Figure 2: Sheet resistances (R_{sheet}) and layer structures according to SEM after exposure to hydrogen plasma, oxygen plasma, and ammoniumthiocyanate solution. Insets in the upper right corners show photographs of the different layers. Gracing incidence X-ray scattering patterns for samples treated with plasma are shown as insets in the lower left corners. SEMs of layers treated for 15 min are shown in Figure S2, supporting information.

the layer. Bundle-like structures remained visible in scanning electron microscopy and the color appeared unchanged to the naked eye (Figure 2). GISAXS confirmed the existence of individual wires after annealing (see inset in Figure 2), and optical UV-Vis transmittance spectra remained largely unchanged (Figures S3, Supporting Information). Interestingly, 1 min of hydrogen plasma exposure decreased the sheet resistance to 200 kΩ/sq, probably by removing a fraction of oleylamine. Sustained exposure to hydrogen plasma caused a significant drop in resistance down to 50 Ω/sq. Thicker bundle-like structures became visible in SEM and indicated sintering of the nanowires. The scattering pattern characteristic for single wires had disappeared from GISAXS after 5 min, and only the Yoneda peak remained.[30] Exposure times above 15 min did not significantly improve conductivity or alter the structure further. The sintering process is probably comparable with the "nanocrystal plasma polymerization" described by Cademartiri and coworkers that removes the capping ligands while retaining the overall nanocrystal arrangement.[31]

Oxygen plasma lowered sheet resistances to values slightly above those found for hydrogen plasma. Sheet resistances remained in the megaohm range after 1 min, dropped to 200 Ω/sq

after 5 min, and to 100 Ω/sq after 15 min. In contrast to hydrogen, oxygen plasma drastically altered the morphology even after short treatments. Only weak X-ray scattering from single wires remained after 1 min (Figure 2), and their scattering was invisible after 5 min annealing time. The changes in the morphology can be attributed to the fact that gold is not inert to the oxygen plasma. The slight oxidation of the surface to Au_2O_3 leads to large compressive stresses induced by the volume change.[32,33]

Ligand exchange only reduced resistance to the megaohm range. Immersion of the layer in an 1% ammoniumthiocyanate solution in acetone for 2 min, as used by Fafarman et al.,[19] led to obvious changes in layer morphology. It appeared to mobilize the wires so that the films underwent morphological changes very different from those observed in gas-phase annealing. Longer immersion led to the formation of coarse agglomerates. An unknown fraction of AuNWs was lost to the solution despite of the adhesion-increasing silanization of the substrates[19] (see experimental details in the SI). Poor reproducibility due to wire loss and the large remaining sheet resistances make ligand exchange by NH_4SCN in acetone less suitable for ultrathin gold wires and will therefore not be considered further here.

Morphology changes induced by annealing can improve or degrade the stability of the conductive layers. We measured the sheet resistances of freshly annealed layers as a function of storage time under ambient conditions (Figure 3). Layers treated with hydrogen and with oxygen plasma aged similarly: the sheet resistances of samples treated for 1 min significantly increased within the first hours, while samples treated for longer times retained their sheet resistances of around 50 Ω/sq (H_2) and 100 Ω/sq (O_2) for at least four months.

The difference in layer stability underpin our interpretation of the annealing mechanism. Rayleigh instability rapidly degraded the original wires with 1.6 nm diameters in days even at room temperature.[27] Figure 4 shows electron micrographs of a sample recorded immediately after layer preparation (a) and after 1 week of storage at ambient conditions (d). Partial fragmentation into spheres is clearly visible and results in a color change from dark-red to blue. Optical spectroscopy shows distinct surface plasmon resonance peaks that are

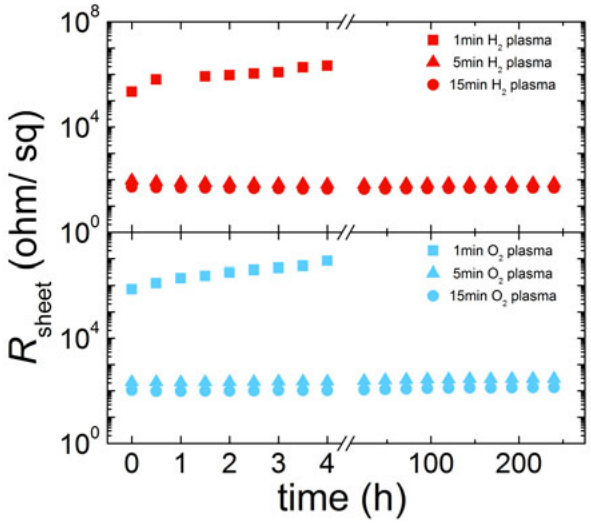

Figure 3: Sheet resistance (R_{sheet}) as a function of storage time after treatment with H_2 plasma and treatment with O_2 plasma. Resistances of layers treated for 1 min exceeded the measurable range after 4 h.

indicative of spheres.

Short plasma treatments did not protect the layers but rather accelerated fragmentation: while untreated layers were stable for days, briefly annealed layers changed their color and sheet resistance already after hours (Figure 3). We believe that oleylamine protects the AuNWs structure, and that its partial removal during a short plasma treatment leads to the acceleration of the fragmentation process. After 1 week, we found only spherical particles (Figures 4e and 4f) with sizes and particle-to-particle distances that were above those expected for the Rayleigh instability, probably indicating Ostwald ripening after fragmentation.[34] The sintered structures that formed after 5 minutes of plasma treatment did not exhibit the Rayleigh instability, and no structural change was observed with time.

In summary, this paper demonstrates that ultrathin gold nanowires become suitable materials for transparent electronics after soft sintering. We dip-coated layers of transparent ultrathin gold wires and found them to be insulating. Layer conductivity was readily increased after removing oleylamine by annealing. Hydrogen low pressure plasma treatment decreased the layers' sheet resistances while retaining optical transmission. Oxygen plasma treatment and solution-based ligand exchange were less effective.

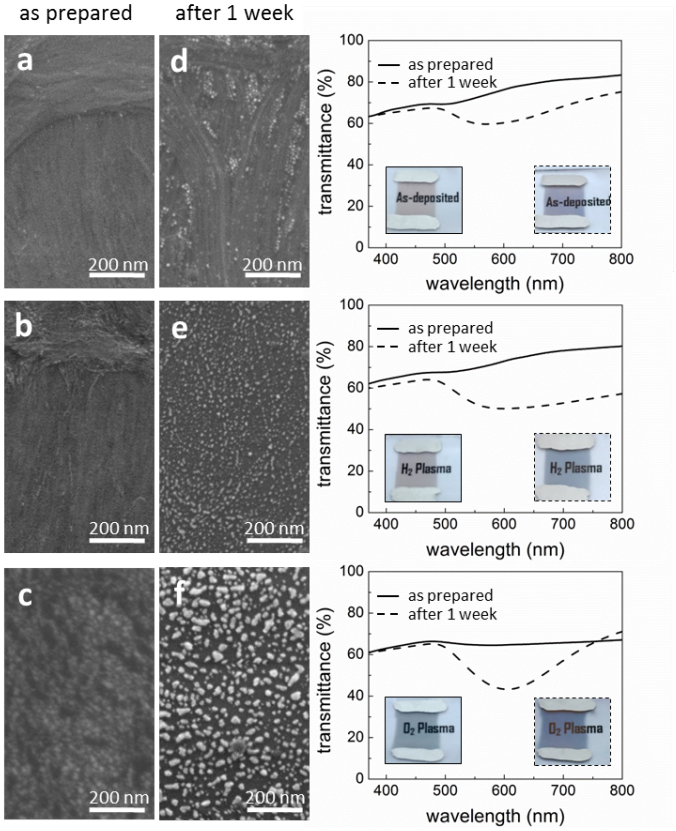

Figure 4: SEM images of AuNW layers recorded directly after (a) layer deposition, (b) 1 min hydrogen plasma treatment and (c) 1 min oxygen plasma treatment. Figures (d-f) on the right-hand side show SEM images of the same samples after 1 week of storage under ambient conditions. The corresponding optical transmittance spectra are displayed on the right with optical photographs of the samples as insets.

Ultrathin AuNWs in freshly prepared layers consistently fragmented after few days at ambient conditions. Partial removal of oleylamine in a short plasma treatment accelerated this degradation. Longer plasma treatments increased layer stability to the point where no degradation was visible even after months. Optimal conditions led to sheet resistances of 50 Ω/sq, similar to a sputtered gold layer with a thickness of around 15 nm.

Annealing seemed to be most effective when it coarsened the layer morphology but retained some of its small-scale features. Electron microscopy and grazing incidence small-angle X-ray scattering indicated sintering of the AuNW into larger, filamentous structures. We believe that the plasma treatment converted nanowire bundles that were already present into stable wires. The sintered wires appear to be thin enough to avoid optical scattering

and retain transparency.

Such "soft sintering" that retains some, but not all features of a microstructure formed in solution is an interesting route to create materials with optimized properties from disperse nanoscale precursors.

Acknowledgement

The authors thank Eduard Arzt for his continuing support of the project. Funding from the German Federal Ministry of Education and Research (BMBF) in the "NanoMatFutur" program is gratefully acknowledged.

Supporting Information Available

Experimental details. Optical transmittance spectra of studied layers. SEM images and GISAXS measurements of samples treated for 15 min. SEM images with different magnifications of samples treated for 5 min in hydrogen plasma.

This material is available free of charge via the Internet at `http://pubs.acs.org/`.

References

(1) De, S.; Higgins, T. M.; Lyons, P. E.; Doherty, E. M.; Nirmalraj, P. N.; Blau, W. J.; Boland, J. J.; Coleman, J. N. Silver Nanowire Networks as Flexible, Transparent, Conducting Films: Extremely High DC to Optical Conductivity Ratios. *ACS Nano* **2009**, *3*, 1767–1774.

(2) Artukovic, E.; Kaempgen, M.; Hecht, D. S.; Roth, S.; Gru, G. Transparent and Flexible Carbon Nanotube Transistors. *Nano Lett.* **2005**, *5*, 757–760.

(3) Wassei, J. K.; Kaner, R. B. Graphene, a Promising Transparent Conductor. *Mater. Today* **2010**, *13*, 52–59.

(4) Kang, M.-G.; Guo, L. Nanoimprinted Semitransparent Metal Electrodes and their Application in Organic Light-Emitting Diodes. *Adv. Mater.* **2007**, *19*, 1391–1396.

(5) Ye, S.; Rathmell, A. R.; Chen, Z.; Stewart, I. E.; Wiley, B. J. Metal Nanowire Networks: The Next Generation of Transparent Conductors. *Adv. Mater.* **2014**, *26*, 6670–6687.

(6) Lee, J.-Y.; Connor, S. T.; Cui, Y.; Peumans, P. Solution-processed Metal Nanowire Mesh Transparent Electrodes. *Nano Lett.* **2008**, *8*, 689–692.

(7) Langley, D.; Giusti, G.; Mayousse, C.; Celle, C.; Bellet, D.; Simonato, J.-P. Flexible Transparent Conductive Materials Based on Silver Nanowire Networks: a Review. *Nanotechnology* **2013**, *24*, 452001.

(8) Rathmell, A. R.; Bergin, S. M.; Hua, Y.-L.; Li, Z.-Y.; Wiley, B. J. The Growth Mechanism of Copper Nanowires and their Properties in Flexible, Transparent Conducting Films. *Adv. Mater.* **2010**, *22*, 3558–3563.

(9) Guo, C. F.; Ren, Z. Flexible Transparent Conductors Based on Metal Nanowire Networks. *Mater. Today* **2014**, *00*, 1–12.

(10) Halder, A.; Ravishankar, N. Ultrafine Single-Crystalline Gold Nanowire Arrays by Oriented Attachment. *Adv. Mater.* **2007**, *19*, 1854–1858.

(11) Wang, C.; Hu, Y.; Lieber, C. M.; Sun, S. Ultrathin Au Nanowires and their Transport Properties. *J. Am. Chem. Soc.* **2008**, *130*, 8902–8903.

(12) Feng, H.; Yang, Y.; You, Y.; Li, G.; Guo, J.; Yu, T.; Shen, Z.; Wu, T.; Xing, B. Simple and Rapid Synthesis of Ultrathin Gold Nanowires, their Self-assembly and Application in Surface-enhanced Raman Scattering. *Chem. Commun.* **2009**, 1984–1986.

(13) Cademartiri, L.; Ozin, G. A. Ultrathin Nanowires-A Materials Chemistry Perspective. *Adv. Mater.* **2009**, *21*, 1013–1020.

(14) Gong, S.; Schwalb, W.; Wang, Y.; Chen, Y.; Tang, Y.; Si, J.; Shirinzadeh, B.; Cheng, W. A Wearable and Highly Sensitive Pressure Sensor with Ultrathin Gold Nanowires. *Nat. Commun.* **2014**, *5*, 1–8.

(15) Chen, Y.; Ouyang, Z.; Gu, M.; Cheng, W. Mechanically Strong, Optically Transparent, Giant Metal Superlattice Nanomembranes from Ultrathin Gold Nanowires. *Adv. Mater.* **2013**, *25*, 80–85.

(16) Sánchez-Iglesias, A.; Rivas-Murias, B.; Grzelczak, M.; Pérez-Juste, J.; Liz-Marzán, L. M.; Rivadulla, F.; Correa-Duarte, M. A. Highly Transparent and Conductive Films of Densely Aligned Ultrathin Au Nanowire Monolayers. *Nano Lett.* **2012**, *12*, 6066–6070.

(17) Lyons, P. E.; De, S.; Elias, J.; Schamel, M.; Philippe, L.; Bellew, A. T.; Boland, J. J.; Coleman, J. N. High-Performance Transparent Conductors from Networks of Gold Nanowires. *J. Phys. Chem. Lett.* **2011**, *2*, 3058–3062.

(18) Hecht, D. S.; Hu, L.; Irvin, G. Emerging Transparent Electrodes Based on Thin Films of Carbon Nanotubes, Graphene, and Metallic Nanostructures. *Adv. Mater.* **2011**, *23*, 1482–1513.

(19) Fafarman, A. T.; Hong, S.-H.; Caglayan, H.; Ye, X.; Diroll, B. T.; Paik, T.; Engheta, N.; Murray, C. B.; Kagan, C. R. Chemically Tailored Dielectric-to-metal Transition for the Design of Metamaterials from Nanoimprinted Colloidal Nanocrystals. *Nano Lett.* **2013**, *13*, 350–357.

(20) Mourdikoudis, S.; Liz-Marzán, L. M. Oleylamine in Nanoparticle Synthesis. *Chem. Mater.* **2013**, *25*, 1465–1476.

(21) Langley, D. P.; Lagrange, M.; Giusti, G.; Jiménez, C.; Bréchet, Y.; Nguyen, N. D.; Bellet, D. Metallic Nanowire Networks: Effects of Thermal Annealing on Electrical Resistance. *Nanoscale* **2014**, *6*, 13535–13543.

(22) Jiang, H.; Vinod, T. P.; Jelinek, R. Spontaneous Assembly of Extremely Long, Horizontally-aligned, Conductive Gold Micro-wires in a Langmuir Monolayer Template. *Adv. Mater. Interfaces* **2014**, 1400187.

(23) Gehl, B.; Frömsdorf, A.; Aleksandrovic, V.; Schmidt, T.; Pretorius, A.; Flege, J.-I.; Bernstorff, S.; Rosenauer, A.; Falta, J.; Weller, H.; Bäumer, M. Structural and Chemical Effects of Plasma Treatment on Close-packed Colloidal Nanoparticle Layers. *Adv. Funct. Mater.* **2008**, *18*, 2398–2410.

(24) Fafarman, A. T.; Koh, W.-k.; Diroll, B. T.; Kim, D. K.; Ko, D.-k.; Oh, S. J.; Ye, X.; Doan-nguyen, V.; Crump, M. R.; Reifsnyder, D. C.; Murray, C. B.; Kagan, C. R. Thiocyanate-Capped Nanocrystal Colloids : Vibrational Reporter of Surface Chemistry and Solution-based Route to Enhanced Coupling in Nanocrystal Solids. *J. Am. Chem. Soc.* **2011**, *133*, 15753–15761.

(25) Rayleigh, L. On the Stability of Jets. *Proc. London Math. Soc.* **1878**, *10*, 4–12.

(26) Toimil Molares, M. E.; Balogh, A. G.; Cornelius, T. W.; Neumann, R.; Trautmann, C. Fragmentation of Nanowires Driven by Rayleigh Instability. *Appl. Phys. Lett.* **2004**, *85*, 5337–5339.

(27) Xu, J.; Zhu, Y.; Zhu, J.; Jiang, W. Ultralong Gold Nanoparticle/Block Copolymer Hybrid Cylindrical Micelles: a Strategy Combining Surface Templated Self-assembly and Rayleigh Instability. *Nanoscale* **2013**, *5*, 6344–6349.

(28) Karim, S.; Toimil-Molares, M. E.; Balogh, A. G.; Ensinger, W.; Cornelius, T. W.; Khan, E. U.; Neumann, R. Morphological Evolution of Au Nanowires Controlled by Rayleigh Instability. *Nanotechnology* **2006**, *17*, 5954–5959.

(29) Loubat, A.; Impéror-Clerc, M.; Pansu, B.; Meneau, F.; Raquet, B.; Viau, G.; Lacroix, L.-M. Growth and self-assembly of ultrathin Au nanowires into expanded hexagonal superlattice studied by in situ SAXS. *Langmuir* **2014**, *30*, 4005–12.

(30) Müller-Buschbaum, P. In *Applications of Synchrotron Light to Scattering and Diffraction in Materials and Life Sciences*; Gomez, M., Nogales, A., Garcia-Gutierrez, M. C., Ezquerra, T., Eds.; Lect. Notes Phys.; Springer Berlin Heidelberg, 2009; Vol. 776; pp 61–89.

(31) Cademartiri, L.; Ghadimi, A.; Ozin, G. A. Nanocrystal Plasma Polymerization : From Colloidal Nanocrystals to Inorganic Architectures. *Acc. Chem. Res.* **2008**, *41*, 1820–1830.

(32) Koslowski, B.; Boyen, H.; Wilderotter, C. Oxidation of preferentially (1 1 1) -oriented Au Films in an Oxygen Plasma Investigated by Scanning Tunneling Microscopy and POotoelectron Spectroscopy. *Surf. Sci.* **2001**, *475*, 1–10.

(33) Fuchs, P. Low-pressure Plasma Cleaning of Au and PtIr Noble Metal Surfaces. *Appl. Surf. Sci.* **2009**, *256*, 1382–1390.

(34) Gentry, S. T.; Kendra, S. F.; Bezpalko, M. W. Ostwald Ripening in Metallic Nanoparticles : Stochastic Kinetics. *J. Phys. Chem. C* **2011**, *115*, 12736–12741.

Graphical TOC Entry

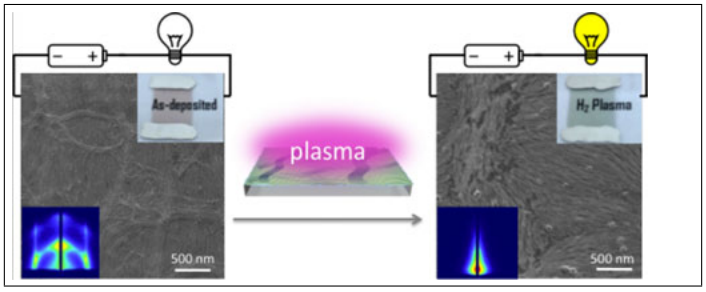

Supporting Information

Sintering of ultrathin gold nanowires for transparent electronics

Johannes H.M. Maurer, Lola González-García,* Beate Reiser, Ioannis Kanelidis,

and Tobias Kraus*

INM - Leibniz Institute for New Materials, Campus D2 2, 66123 Saarbrücken, Germany

E-mail: lola.gonzalez-garcia@inm-gmbh.de; tobias.kraus@inm-gmbh.de

*To whom correspondence should be addressed

Methods

All chemicals were obtained from the denoted sources and used without further purification. Chloroauric acid was prepared by dissolving a gold ingot (999.9 Degussa, München, Germany) in aqua regia.

Ultrathin gold nanowires were synthesized according to a recipe published by Feng et al.[1] The concentration of gold was scaled up to 8 times compared to the original procedure. In a typical synthesis, 39 mg of $HAuCl_4xH_2O$ were dissolved in a mixture of 5.8 ml of n-hexane (99%, ABCR, Germany) and 1.7 ml of oleylamine (technical grade, 70%, Sigma-Aldrich, Steinheim, Germany) to result in a dark yellow solution. 1.5 ml of triisopropylsilane (98%, ABCR, Germany) were added and the solution was stirred vigorously for 30 s. Afterwards the reaction mixture was flushed with argon and kept undisturbed at RT overnight. The wires were precipitated by adding ethanol (2.5 times the reaction volume). The supernatant was carefully removed and the wires were redispersed in n-hexane. The washing step was repeated once. Homogeneous and dense layers of AuNWs with 10 nm thicknesses were prepared on glass microscope slides (Paul Marienfeld GmbH & Co. KG, Lauda-Königshofen, Germany) by dip-coating. The glass slides were dipped manually into the nanowires solution (2 mg/ml of gold) and the process was repeated 5 times. To ensure comparable layer thickness, all samples were checked by UV-vis spectroscopy in transmission mode. Prior to layer formation, the glass slides were thoroughly cleaned using ultrasonication in different solvents: Milli-Q water, ethanol:acteone (1:1 v/v). After each sonication step, the glass slides were rinsed with the corresponding solvents and dried under nitrogen. After that, the glass slides were treated with oxygen plasma for 5 min and silanized by immersion in 5% 3-

mercaptopropyltrimethoxysilane (95%, Sigma-Aldrich, Steinheim, Germany) in toluene overnight according to published procedure.[2]

Annealing

Plasma treatments were performed in a RF PICO plasma system (Diener electronic GmbH & Co. KG, Ebhausen, Germany) operating at 0.3 mbar, 100 W either using 100% oxygen or a 5% hydrogen mixture with argon. For the ligand exchange, the substrates with the AuNW layers were immersed in 1% NH_4SCN (>97%, Sigma-Aldrich, Steinheim, Germany) in acetone for different times, followed by cleaning in pure acetone as reported in literature.[2,3]

Characterization

Single AuNWs were characterized by Transmission Electron Microscopy (JEM 2010, JEOL, Germany) operating at 200 kV. The morphology of the AuNW layers was characterized by Scanning Electron Microscopy (Quanta 400 ESEM, FEI, Germany). Optical characterization was performed by UV-vis spectroscopy in transmission mode (Cary 5000, Varian). GISAXS measurements were carried out on a Xeuss 2.0 system (Xenocs SA, Grenoble, France) with a micro-focused sealed tube Cu Kα X-ray source (λ = 0.154 nm) operating at 50 kV and 0.6 mA and a Hybrid Photon Counting detector (PILATUS 1M, DECTRIS, Baden, Switzerland). The sample-detector distance was 1224.64 mm. The GISAXS pattern presented in the figures were acquired using 0.4° as incident angle. Measurements at higher incident angles did not present any differences revealing the complete probing of the entire film thickness. The sheet resistance of the layers was carried out using a multimeter. Contacts were made of silver paint defining an area of 0.75x0.75 cm^2.

Supporting Figures

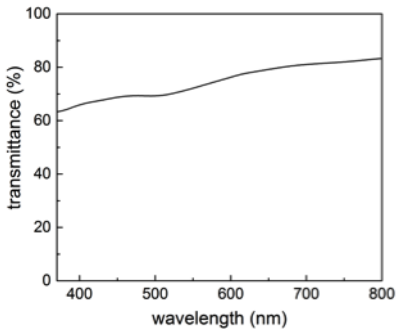

Figure S1: Optical transmittance spectrum of an as-deposited AuNW layer on glass.

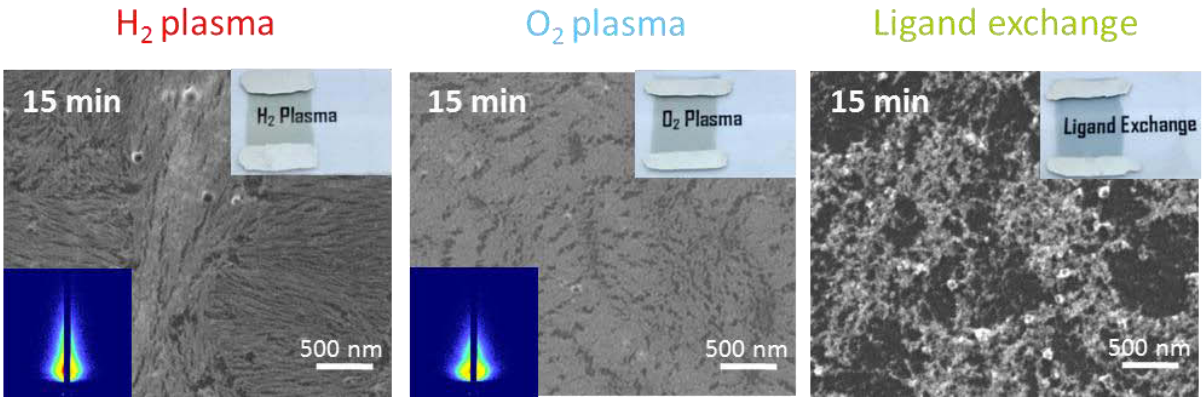

Figure S2: Scanning Electron Micrographs of AuNW layers treated for 15 min with hydrogen plasma, oxygen plasma, and ammoniumthiocyanate solution. Insets in the upper right corners show photographs of the different layers. Gracing incidence small-angle X-ray scattering patterns for samples treated with plasma are shown as insets in the lower left corners.

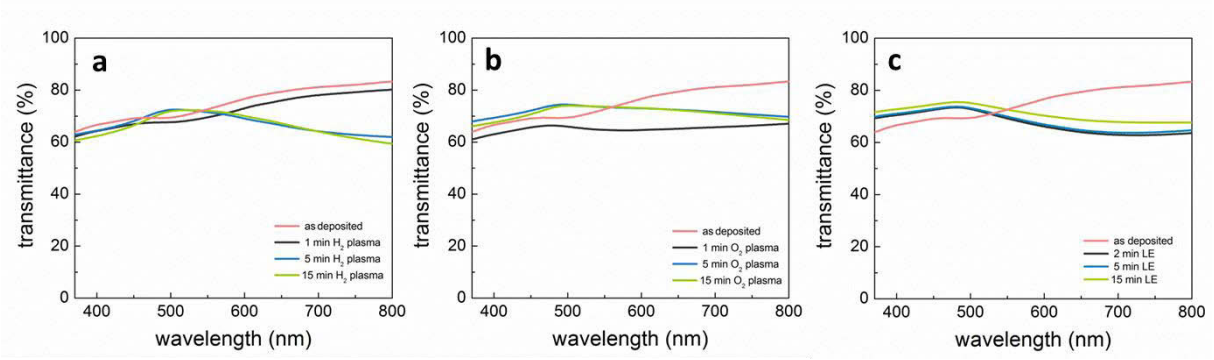

Figure S3: Optical transmittance spectra of AuNW layers on glass for (a) treatment with hydrogen plasma, (b) treatment with oxygen plasma, and (c) ligand exchange.

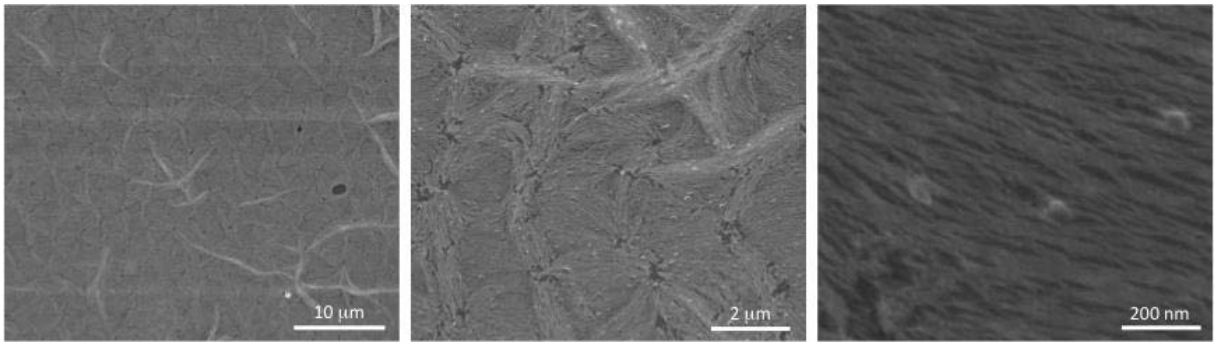

Figure S4: Scanning electron micrographs at different magnification of the sample treated 5 min with hydrogen plasma.

References

(1) Feng, H.; Yang, Y.; You, Y.; Li, G.; Guo, J.; Yu, T.; Shen, Z.; Wu, T.; Xing, B. Simple and Rapid Synthesis of Ultrathin Gold Nanowires, their Self-assembly and Application in Surface-enhanced Raman Scattering *Chem. Commun.* **2009**, 1984-1986.

(2) Fafarman, A. T.; Hong, S.-H.; Caglayan, H.; Ye, X.; Diroll, B. T.; Paik, T.; Engheta, N.; Murray, C. B.; Kagan, C. R. Chemically Tailored Dielectric-to-metal Transition for the Design of Metamaterials from Nanoimprinted Colloidal Nanocrystals *Nano Lett.* **2013**, *13*, 350-357.

(3) Fafarman, A. T.; Koh, W.-K.; Diroll, B. T.; Kim, D. K.; Ko, D.-K.; Oh, S. J.; Ye, X.; Doan-nguyen, V.; Crump, M. R.; Reifsnyder, D. C.; Murray, C. B.; Kagan, C. R. Transparent and Flexible Carbon Nanotube Transistors *J. Am. Chem. Soc.* **2011**, *133*, 15753-15761.